Sensitization of spinal itch transmission neurons in a mouse model of chronic itch requires an astrocytic factor

Keisuke Koga, PhD,* Ryo Yamagata, MS,* Keita Kohno, DS, Takuya Yamane, MPharm, Miho Shiratori-Hayashi, PhD, Yuta Kohro, PhD, Hidetoshi Tozaki-Saitoh, PhD, and Makoto Tsuda, PhD *Fukuoka, Japan*

GRAPHICAL ABSTRACT

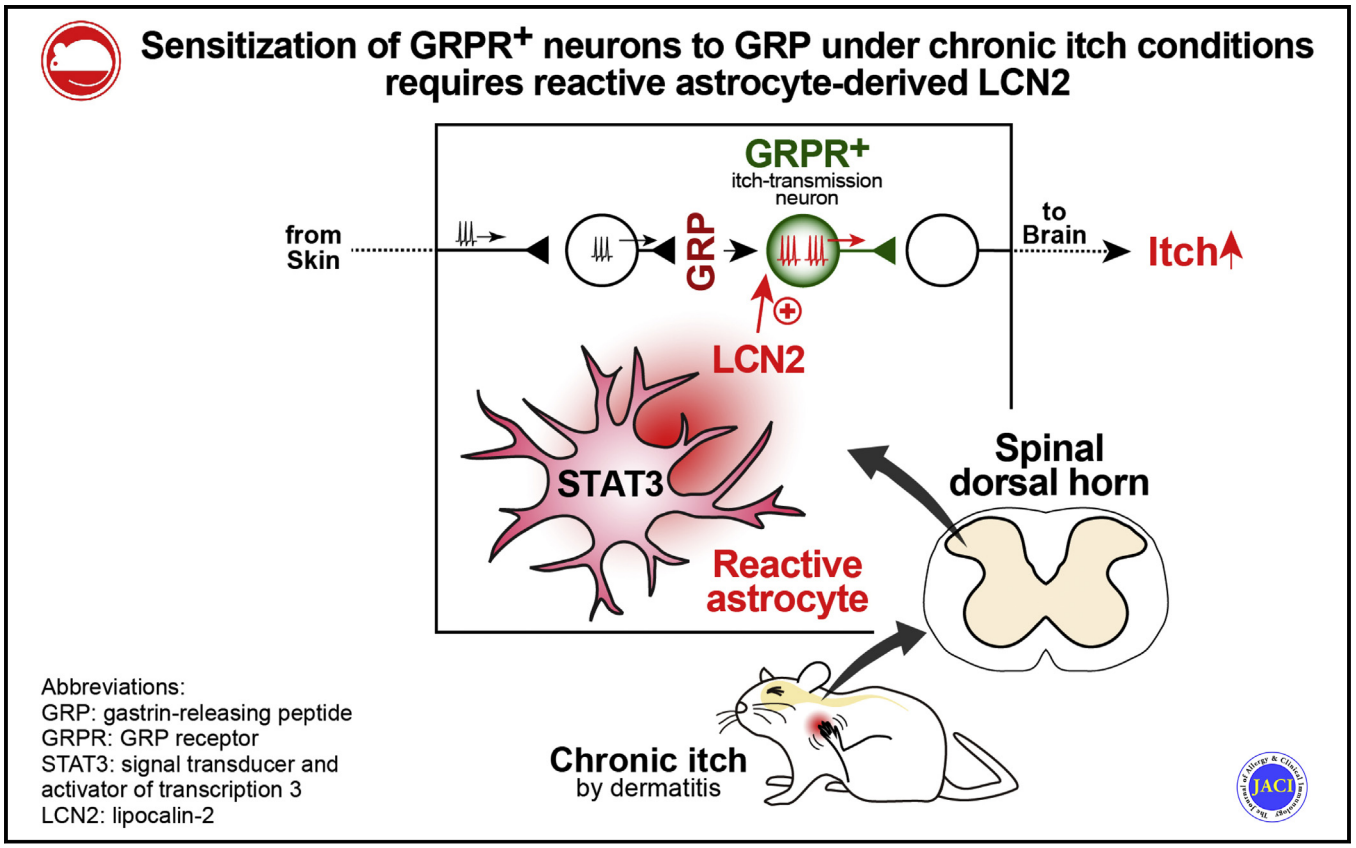

Background: Chronic itch is a highly debilitating symptom among patients with inflammatory skin diseases. Recent studies have revealed that gastrin-releasing peptide (GRP) and its receptor (gastrin-releasing peptide receptor [GRPR]) in the spinal dorsal horn (SDH) play a central role in itch transmission.

Objective: We aimed to investigate whether GRP-GRPR signaling is altered in SDH neurons in a mouse model of chronic itch and to determine the potential mechanisms underlying these alterations.

Methods: Patch-clamp recordings from enhanced green fluorescent protein (EGFP)–expressing ($GRPR^+$) SDH neurons

From the Department of Life Innovation, Graduate School of Pharmaceutical Sciences, Kyushu University.

*These authors contributed equally to this work.

This work was supported by JSPS KAKENHI grants JP15H02522, JP19K22500, and JP19H05658 (to M.T.), by the Core Research for Evolutional Science and Technology (CREST) program from Japan Agency for Medical Research and Development (AMED) under grant number JP19gm0910006 (to M.T.), by the Practical Research Project for Allergic Diseases and Immunology (Research on Allergic Diseases and Immunology) from AMED under grant number JP18ek0410034 (to M.T.), and by the Platform Project for Supporting Drug Discovery and Life Science Research (Basis for Supporting Innovative Drug Discovery and Life Science Research [BINDS]) from AMED under grant number JP19am0101091 (to M.T.).

Disclosure of potential conflict of interest: The authors declare that they have no relevant conflicts of interest.

Received for publication April 25, 2019; revised August 16, 2019; accepted for publication September 26, 2019.

Corresponding author: Makoto Tsuda, PhD, Department of Life Innovation, Graduate School of Pharmaceutical Sciences, Kyushu University, 3-1-1 Maidashi, Higashi-ku, Fukuoka 812-8582, Japan. E-mail: tsuda@phar.kyushu-u.ac.jp.

The CrossMark symbol notifies online readers when updates have been made to the article such as errata or minor corrections

0091-6749/$36.00

https://doi.org/10.1016/j.jaci.2019.09.034

were used to examine GRP-GRPR signaling in spinal cord slices obtained from *Grpr-EGFP* mice. Immunohistochemical, genetic (gene expression and editing through adeno-associated virus vectors), and behavioral approaches were also used for *in vivo* experiments.

Results: We observed potentiation of GRP-evoked excitation in the GRPR$^+$ SDH neurons of mice with contact dermatitis, without concomitant changes in GRPR expression. Interestingly, increases in excitation were attenuated by suppressing the reactive state of SDH astrocytes, which are known to be reactive in patients with chronic itch conditions. Furthermore, CRISPR-Cas9–mediated astrocyte-selective *in vivo* editing of a gene encoding lipocalin-2 (LCN2), an astrocytic factor implicated in chronic itch, suppressed increases in GRP-induced excitation of GRPR$^+$ neurons, repetitive scratching, and skin damage in mice with contact dermatitis. Moreover, LCN2 potentiated GRP-induced excitation of GRPR$^+$ neurons in normal mice.

Conclusion: Our findings indicate that, under chronic itch conditions, the GRP-induced excitability of GRPR$^+$ SDH neurons is enhanced through a non–cell-autonomous mechanism involving LCN2 derived from reactive astrocytes. (J Allergy Clin Immunol 2020;145:183-91.)

Key words: *Contact dermatitis, chronic itch, gastrin-releasing peptide, gastrin-releasing peptide receptor, spinal dorsal horn neurons, astrocytes, lipocalin 2, CRISPR-Cas9, patch-clamp recordings*

Abbreviations used

AAV:	Adeno-associated virus
ACSA-2:	Anti-astrocyte cell-surface antigen 2
aCSF:	Artificial cerebrospinal fluid
DCP:	Diphenylcyclopropenone
dnSTAT3:	Dominant negative form of STAT3
EGFP:	Enhanced green fluorescent protein
GFAP:	Glial fibrillary acidic protein
GRP:	Gastrin-releasing peptide
GRPR:	Gastrin-releasing peptide receptor
LCN2:	Lipocalin-2
SaCas9:	*Staphylococcus aureus* Cas9
sgLcn2:	*Lcn2*-targeting single-guide RNA expression cassette
SDH:	Spinal dorsal horn
STAT3:	Signal transducer and activator of transcription 3
TEWL:	Transepidermal water loss
wtSTAT3:	Wild-type STAT3

Itch is defined as an unpleasant cutaneous sensation that provokes the desire to scratch.[1] This sensation generally serves as a warning or mechanism of self-protection against harmful external agents, and scratching can transiently relieve such itching sensations. However, intense chronic itching occurs in multiple dermatologic inflammatory diseases (eg, atopic and contact dermatitis), leading to excessive repetitive scratching that worsens skin damage and inflammation. Therefore it remains necessary to elucidate the mechanisms underlying this symptom to promote the development of novel therapeutic agents for chronic itch.

Similar to other types of somatosensory information (eg, tactile/pain), itch information is conveyed through primary afferents from the skin to the spinal dorsal horn (SDH), where it is processed by complex neural circuits.[2] Accumulating evidence has demonstrated the existence of neuronal circuits in the SDH involved selectively in itch processing and transmission.[2-4] In particular, previous studies have indicated that the endogenous neuropeptide gastrin-releasing peptide (GRP) induces itch-related behaviors.[5] Indeed, intrathecal administration of GRP induces robust scratching through gastrin-releasing peptide receptors (GRPRs), and mice lacking GRPR exhibit reduced scratching responses evoked by intradermal injection of pruritogens without alterations in pain, thermal, or mechanical sensation.[5] GRPRs are expressed in a subset of SDH neurons (GRPR$^+$), and ablating these neurons suppresses itch-related behaviors.[6] Thus GRPR$^+$ neurons in the SDH can serve as a hub in the processing of itch signals from the skin.[7] Furthermore, loss of GRPR[8] or GRPR$^+$ neurons[6] suppresses repetitive scratching behaviors in mouse models of chronic itch, suggesting that GRP-GRPR signaling in SDH neurons is also involved in chronic itch. However, whether chronic itch is associated with altered GRP-GRPR signaling in SDH neurons remains to be determined.

In the present study we aimed to investigate whether such signaling is altered in a mouse model of chronic itch and to determine the potential mechanisms underlying these alterations. Our findings indicated that GRP-induced excitability of GRPR$^+$ SDH neurons is potentiated in a mouse model of chronic itch and that this hyperexcitability requires a non–cell-autonomous signal from SDH astrocytes, glial cells that are activated under chronic itch conditions.[9]

METHODS

Additional details are presented in the Methods section in this article's Online Repository at www.jacionline.org.

Animals

Male *Grpr-EGFP* mice (STOCK Tg[Grpr-EGFP]PZ62Gsat/Mmucd) and wild-type ICR mice (CLEA, Tokyo, Japan) were used.

Recombinant adeno-associated virus vector production

We made the following adeno-associated virus (AAV) vectors to express genes of interest in SDH astrocytes (AAV-gfaABC$_1$D-mCherry, AAV-gfaABC$_1$D-dominant negative form of signal transducer and activator of transcription 3 [dnSTAT3] or AAV-gfaABC$_1$D-wild-type STAT3 [wtSTAT3]). For CRISPR-Cas9–mediated lipocalin-2 (LCN2) knockout, AAV-gfaABC$_1$D-SaCas9 and AAV-gfaABC$_1$D-mCherry-U6-sgRNA were made.

Microinjection of recombinant AAV into the cervical SDH

Mice were deeply anesthetized, and the glass microcapillary was inserted into the SDH (150-200 μm in depth from the surface of the dorsal root entry zone) with a preflow of recombinant AAV solution through an interspace between C3 and C4 vertebrae by using Micro Syringe Pumps (SYS-micro4; World Precision Instruments, Sarasota, Fla).

Immunohistochemistry

As we previously reported,[9] transverse spinal cord (C3-C5 segments) sections were used.

Electrophysiology

Whole-cell patch-clamp recordings were performed in enhanced green fluorescent protein (EGFP)$^+$ SDH neurons by using spinal cord slices. GRP (50 or 300 nmol/L), LCN2 (10 nmol/L), or both were applied to the slices.

Mouse model of chronic itch

Mice were shaved on the back and received topically applied diphenylcyclopropenone (DCP; dissolved in acetone) to induce contact dermatitis. Seven days after the first painting, DCP was painted again on the same area of skin. Transepidermal water loss (TEWL) was also measured.

Real-time RT-PCR

As we previously reported,[9] total RNA extracts from the C3-C5 segments of the spinal cord were used.

Measurement of scratching behavior

Scratching behavior in mice was automatically detected and objectively evaluated by using automated scratching analysis system (MicroAct; Neuroscience, Tokyo, Japan), as described previously.[9]

DNA extraction and assessment of *in vivo* genome editing

DNA extracts from sorted astrocytes were used for assessing *in vivo* genome editing by using a resolvase-based mutation detection kit.

Statistical analysis

All data are shown as means ± SEMs. Statistical significance of differences was determined by using the paired *t* test, the unpaired *t* test, the unpaired *t* test with the Welch correction, the Mann-Whitney test, 2-way repeated-measures ANOVA with the *post hoc* Bonferroni test, and 1-way ANOVA with the *post hoc* Tukey multiple comparisons test by using GraphPad Prism 4 and 7 software (GraphPad Software, La Jolla, Calif). Differences were considered significant at a P value of less than .05.

RESULTS

GRPR$^+$ neurons in the cervical SDH are mainly excitatory

To visualize GRPR$^+$ SDH neurons, we used *Grpr-EGFP* mice, in which EGFP is expressed in neurons under the control of the GRPR promotor.[8] In the SDH EGFP fluorescence was observed in the superficial laminae (I-II; Fig 1, *A*), which is consistent with previous results.[8,10] Whole-cell patch-clamp recordings were obtained from EGFP$^+$ SDH neurons in spinal cord slices taken from *Grpr-EGFP* mice. GRP produced excitation of these SDH neurons (Fig 1, *B*), confirming the expression of functional GRPR in EGFP$^+$ neurons. Furthermore, to determine whether GRPR$^+$ SDH neurons are excitatory or inhibitory, we examined the pattern of action potential firing generated by adding a depolarizing current to EGFP$^+$ SDH neurons at the resting membrane potential because excitatory and inhibitory SDH neurons have been shown to display distinct types of firing patterns.[11] We found that 80.4% of EGFP$^+$ neurons exhibited a delayed (38/56 neurons) or transient (7/56 neurons) firing pattern (Fig 1, *C*), both of which are known as an electrophysiologic criterion for excitatory neurons.[11] Other EGFP$^+$ neurons (11/56 neurons) exhibited a tonic firing pattern (Fig 1, *C*), which is observed in inhibitory neurons.[11] GRP-induced depolarization was greater in EGFP$^+$ neurons exhibiting a delayed firing pattern than in those exhibiting a transient firing pattern (delayed type, 10.35 ± 1.48 [n = 10]; transient type, 5.03 ± 1.74 [n = 5]; $P < .05$, unpaired *t* test), and the number of neurons generating action potentials was also greater in neurons exhibiting a delayed firing pattern (delayed type, 8/10 neurons; transient type, 0/5 neurons). Morphologically, 83% of EGFP$^+$ neurons exhibiting a delayed firing pattern (20/24 cells) had ventrally directed dendrites (Fig 1, *D*), which appeared to be vertical-type neurons, axons of which are known to arborize to more superficial regions of lamina I that project to the brain.[12] Moreover, 76.4% of EGFP$^+$ SDH neurons were not immunolabeled with paired box 2 (298/390 neurons, 4 mice; Fig 1, *E*), a marker of inhibitory interneurons.[13,14] These results indicate that EGFP$^+$ neurons exhibiting a delayed firing pattern are excitatory and thus more sensitive to GRP. Therefore we analyzed these neurons (hereafter referred to as GRPR$^+$ neurons) in subsequent electrophysiologic experiments.

GRP-evoked excitation in GRPR$^+$ neurons is enhanced in a mouse model of chronic itch

To examine whether GRP-induced excitation of GRPR$^+$ SDH neurons is altered under chronic itch conditions, we treated *Grpr-EGFP* mice with DCP, a reagent known to produce chronic itch related to contact dermatitis.[15] DCP-treated *Grpr-EGFP* mice exhibited spontaneous repetitive scratching behavior (Fig 2, *A*), dermatitis (Fig 2, *B*), and an increase in TEWL (an index of skin barrier dysfunction; Fig 2, *C*). In spinal cord slices obtained from these mice, application of GRP (50 nmol/L) induced greater depolarization of the membrane potential in GRPR$^+$ neurons than that observed in naive[10] and acetone-treated control mice (Fig 2, *D* and *E*). GRP (50 nmol/L) also generated action potentials in 9 of 12 GRPR$^+$ SDH neurons obtained from DCP-treated mice (Fig 2, *D*), and this number was much greater than that in acetone-treated control mice (2/12 neurons). Resting membrane potentials were indistinguishable between the DCP-treated and control groups (Fig 2, *F*). These data indicate that GRP-induced increases in the excitability of GRPR$^+$ SDH neurons are enhanced in a mouse model of chronic itch associated with contact dermatitis.

Sensitization of GRP-GRPR signaling under chronic itch conditions requires reactive astrocytes

We explored the mechanisms underlying increases in GRP-induced excitation of GRPR$^+$ SDH neurons. Our quantitative PCR analysis revealed no increases in expression of *Grpr* or *Grp* mRNA in the spinal cords of DCP-treated mice (see Fig E1, A and B, in this article's Online Repository at www.jacionline.org). In addition, mRNA levels for natriuretic polypeptide B (an activator of GRP$^+$ SDH neurons[16]) in the dorsal root ganglia were not changed in DCP-treated mice (see Fig E1, *C*). These results suggest that increases in GRP-evoked excitation are not simply caused by changes in expression of GRPR and its ligand but also by pathologic signaling alterations in the SDH.

We then examined the role of astrocytes because these cells become reactive in the SDH of mice with atopic and contact dermatitis, playing a pivotal role in chronic itch.[9] The reactive state of SDH astrocytes is regulated by the transcription factor signal transducer and activator of transcription 3 (STAT3).[17] Therefore we injected the cervical SDH with AAV vectors containing the astrocyte-specific promoter gfaABC$_1$D,[18,19]

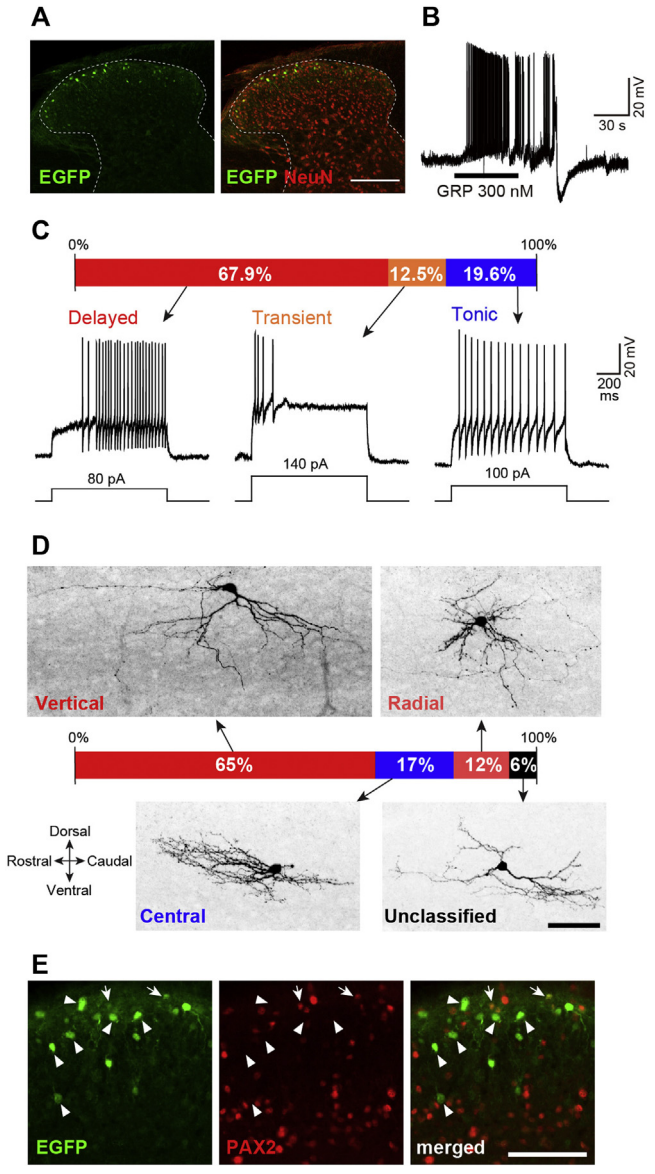

FIG 1. Characterization of EGFP$^+$ neurons in the SDH of *Grpr-EGFP* mice. **A,** EGFP fluorescence (green) in the SDH of *Grpr-EGFP* mice. Neuronal nuclei (*NeuN*; red) are markers of neurons. *Scale bar* = 200 μm. **B,** Representative response of GRP (300 nmol/L) in EGFP$^+$ SDH neurons (displaying the delayed firing pattern). **C,** Firing patterns of EGFP$^+$ SDH neurons and percentages of neurons displaying each pattern. **D,** Representative confocal images for the morphology of EGFP$^+$ neurons in the SDH. *Scale bar* = 100 μm. **E,** Immunohistochemical identification of EGFP$^+$ neurons by using paired box 2 *(PAX2)* staining (red), a marker of inhibitory interneurons. *Arrows* and *arrowheads* indicate PAX2-positive and PAX2-negative EGFP$^+$ neurons, respectively. *Scale bar* = 100 μm.

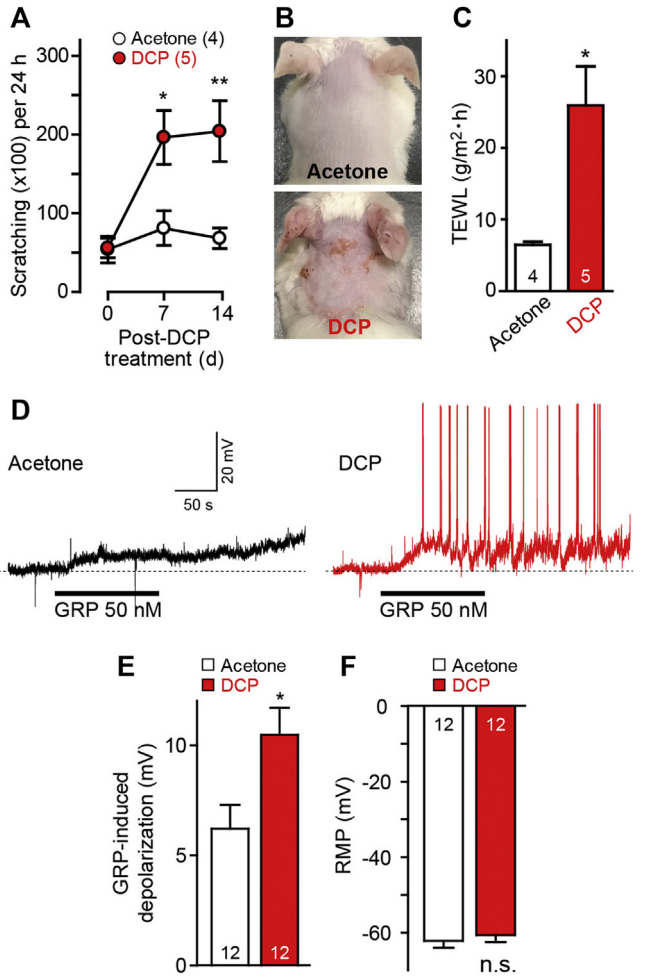

FIG 2. Enhancement of GRP-induced excitation of GRPR$^+$ SDH neurons under chronic itch conditions. **A,** Number of scratching behaviors during 24 hours of acetone- or DCP-treated *Grpr-EGFP* mice at days 0, 7, and 14. *P < .05 and **P < .01 versus the acetone group. **B,** Dermatitis of the rostral back skin of acetone- or DCP-treated *Grpr-EGFP* mice at day 14. **C,** TEWL of the rostral back skin in acetone- or DCP-treated *Grpr-EGFP* mice at day 14. *P < .05. **D-F,** GRP-induced depolarization (Fig 2, *D*: representative traces; Fig 2, *E*: summary data; *P < .05) and resting membrane potentials (*RMP* [in millivolts]; Fig 2, *F*) of GRPR$^+$ neurons in the SDH of acetone- or DCP-treated *Grpr-EGFP* mice (days 13 or 14).

suppressing the reactive state of SDH astrocytes through expression of a dominant negative form of STAT3 (dnSTAT3; Fig 3, *A*).[20] In mice with AAV-mCherry (control), almost all mCherry$^+$ cells were immunostained with glial fibrillary acidic protein (GFAP; Fig 3, *B*), which is indicative of selective gene expression in cervical SDH astrocytes. Expression of AAV-dnSTAT3 suppressed DCP-induced increases in GFAP immunofluorescence (an index of reactive astrocytes; Fig 3, *C*), and the intensity of GFAP immunofluorescence was significantly reduced (Fig 3, *D*). Increases in GRP-induced excitation of GRPR$^+$ SDH neurons were prevented in spinal cord slices obtained from DCP-treated *Grpr-EGFP* mice with AAV-dnSTAT3 (Fig 3, *E*), and the decrease in GRP-induced depolarization was statistically significant (Fig 3, *F*). However, dnSTAT3 did not alter the resting membrane potential of GRPR$^+$ neurons (see Fig E2, *A*, in this article's Online Repository at www.jacionline.org) or *Grpr* mRNA levels in the spinal cord (see Fig E2, *B*). In addition, astrocytic dnSTAT3 expression had no effect on GRP-evoked depolarization in GRPR$^+$ neurons in normal *Grpr-EGFP* mice (see Fig E3, *A*, in this article's Online Repository at www.jacionline.org) and on scratching and TEWL in acetone-treated mice (see Fig E3, *B* and *C*). Consistent with attenuation of GRP-induced neuronal excitation by dnSTAT3, astrocytic expression of dnSTAT3 in DCP-treated mice significantly suppressed an increase in c-Fos expression (a marker of neuronal activation) in the superficial SDH (lamina I–II; Fig 3, *G*) and scratching

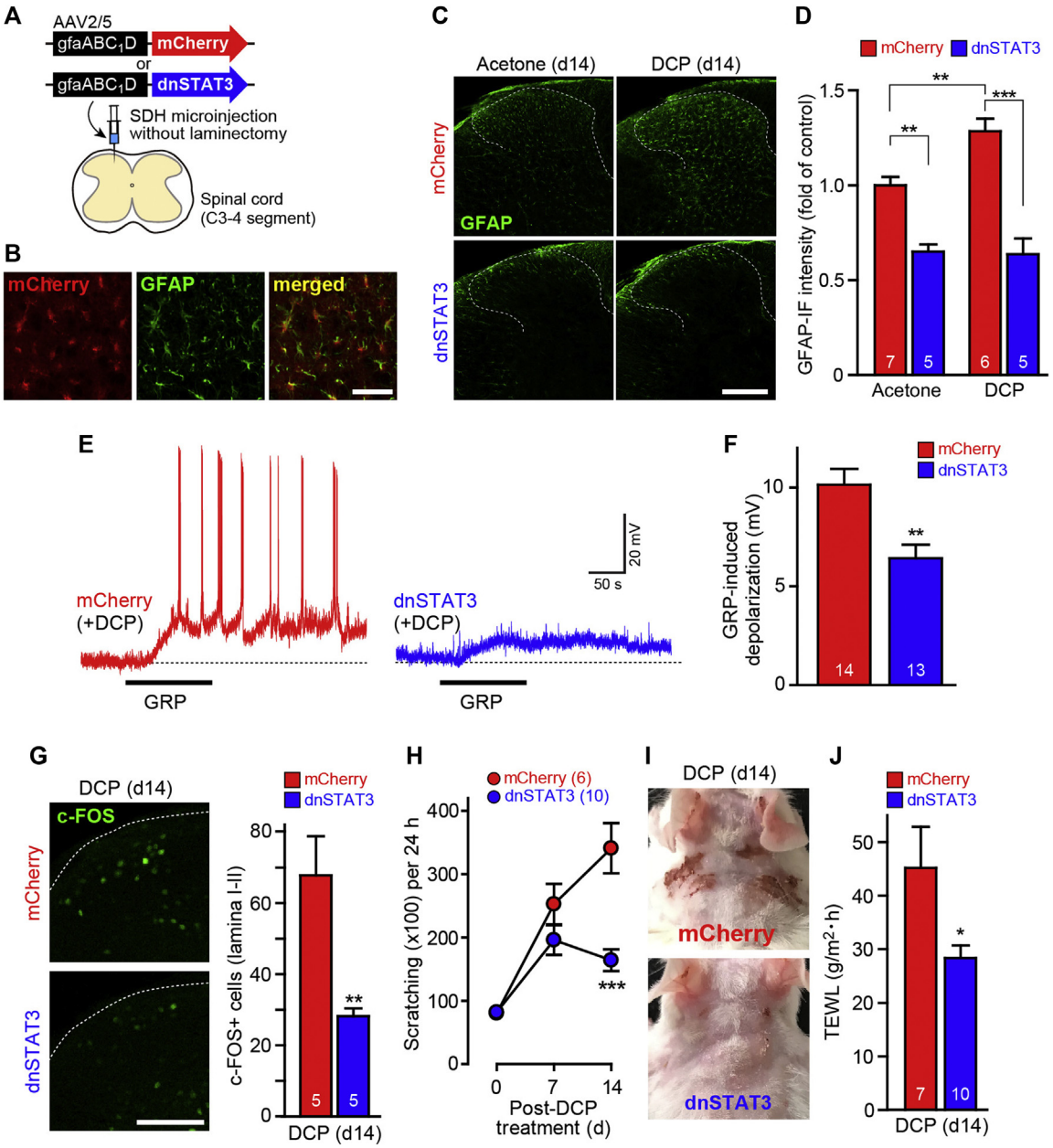

FIG 3. Involvement of reactive astrocytes in the sensitization of GRPR$^+$ SDH neurons. **A,** Schematic illustration of AAV vector constructs designed to express mCherry or dnSTAT3 under the control of an astrocyte-selective promoter (gfaABC$_1$D). **B,** Confocal images of mCherry$^+$ astrocytes (red) in the SDH (green; GFAP). *Scale bar* = 50 μm. **C** and **D,** Effect of dnSTAT3 on GFAP expression in the cervical SDH of acetone- or DCP-treated mice (day 14). Representative images of GFAP immunofluorescence (Fig 3, *C*: *scale bar* = 200 μm) and quantification of GFAP immunofluorescence *(IF)* intensity (Fig 3, *D*: $^{**}P < .01$ and $^{***}P < .001$). **E** and **F,** GRP-induced depolarization of GRPR$^+$ SDH neurons in DCP-treated *Grpr-EGFP* mice with AAV-mCherry or dnSTAT3 at days 13 or 14 (Fig 3, *E*: representative traces; Fig 3, *F*: averaged data; $^{**}P < .01$). **G,** Effect of dnSTAT3 on numbers of c-Fos$^+$ SDH neurons in acetone- or DCP-treated mice. Representative images (*left*; *scale bar* = 100 μm) and averaged data ($^{**}P < .01$) are shown. **H,** Effect of dnSTAT3 on DCP-induced scratching behavior. $^{***}P < .001$. **I** and **J,** Effect of dnSTAT3 on rostral back skin dermatitis (Fig 3, *I*) and TEWL in DCP-treated mice (Fig 3, *J*). $^{*}P < .05$.

behavior (Fig 3, *H*), skin lesioning (Fig 3, *I*), and TEWL (Fig 3, *J*) relative to findings observed in DCP-treated mCherry mice.

As an additional control group, we tested DCP-treated mice whose SDH astrocytes expressed wtSTAT3. Compared with mCherry-expressing DCP-treated mice, wtSTAT3 did not affect the GRP-evoked depolarization (see Fig E4, *A* and *B*, in this article's Online Repository at www.jacionline.org) and the resting membrane potential of GRPR$^+$ neurons on day 14 (see Fig E4, *C*). wtSTAT3 did not significantly affect (but tended to increase) the DCP-induced scratching on day 14 (although wtSTAT3 significantly increased on day 7; see Fig E4, *D*). TEWL and spinal *Grpr* mRNA expression were not altered in

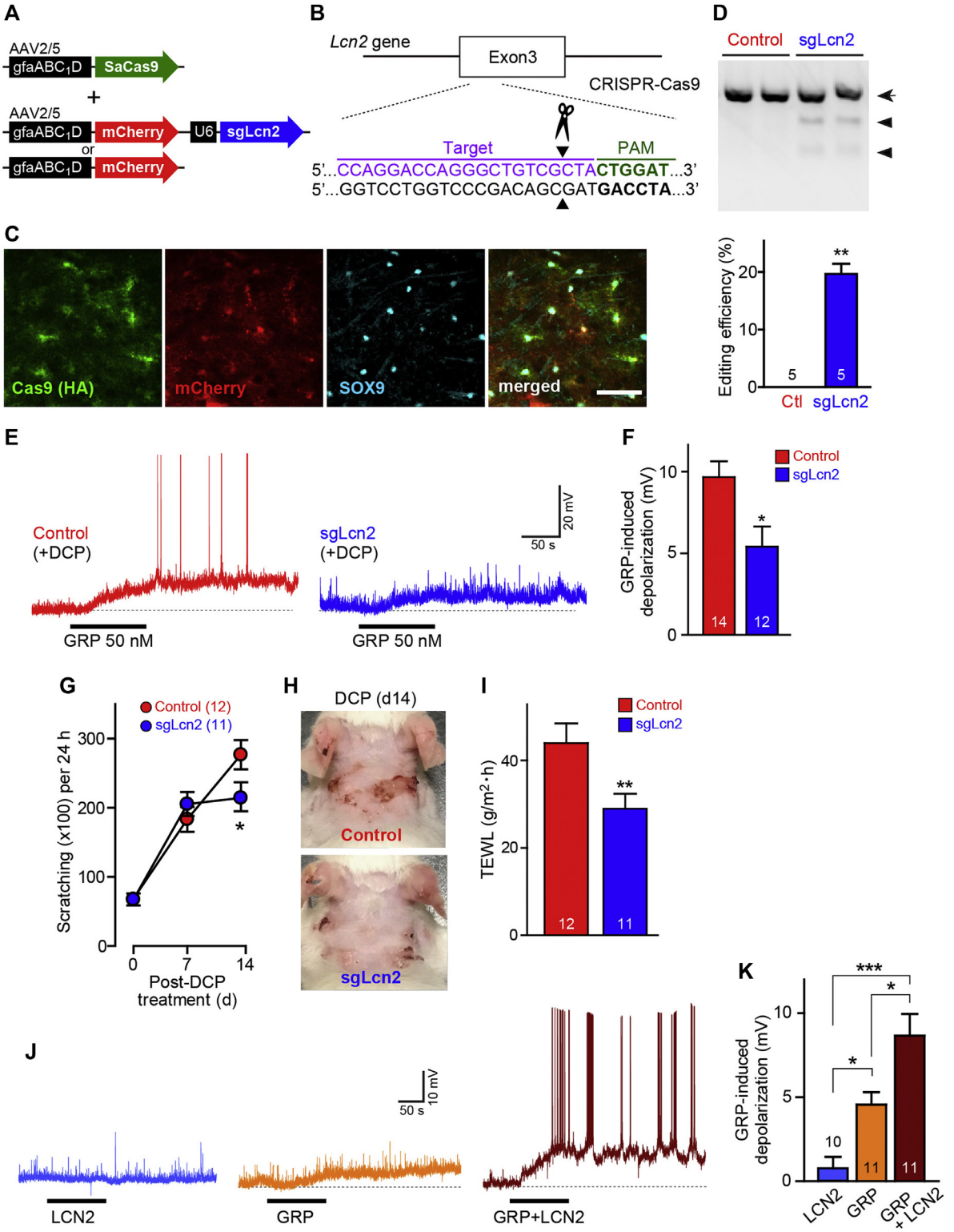

FIG 4. Attenuation of GRPR$^+$ neuron sensitization through AAV–CRISPR-Cas9–mediated editing of the astrocytic *Lcn2* gene. **A** and **B,** Schematic illustrations of AAV vector constructs containing SaCas9 or mCherry (alone [control] or fused with sgLcn2) with the gfaABC$_1$D promoter (Fig 4, *A*) and sgLcn2 binding site (target) in the *Lcn2* locus (Fig 4, *B*). *PAM*, Protospacer adjacent motif. *Triangles* indicate sites of cleavage. **C,** Confocal images of SaCas9 (HA-tag, green)– and mCherry (red)–expressing astrocytes in the SDH 10 weeks after AAV microinjection. SOX9 is a marker of astrocytes (blue). *Scale bar* = 50 μm. **D,** Gel image for detection of genome editing in sorted SDH astrocytes *(upper)* and quantified results *(lower)*. $^{**}P < .01$. *Arrow*, Uncleaved *Lcn2* DNA; *arrowheads*, cleaved *Lcn2* DNA. **E** and **F,** GRP-induced depolarization of GRPR$^+$ neurons in DCP-treated *Grpr-EGFP* mice with AAV-mCherry or sgLcn2 at days 13 or 14 after the DCP application. Representative traces (Fig 4, *E*) and averaged data (Fig 4, *F*) are shown. $^{*}P < .05$. **G–I,** Effect of *Lcn2* genome editing on DCP-induced scratching (Fig 4, *G*; $^{*}P < .05$ vs the control group), dermatitis (Fig 4, *H*), and TEWL at day 14 (Fig 4, *I*; $^{**}P < .01$). **J** and **K,** Effect of coapplication of LCN2 (10 nmol/L) on GRP-induced depolarization of GRPR$^+$ neurons in naive *Grpr-EGFP* mice. Representative traces (Fig 4, *J*) and averaged data (Fig 4, *K*) are shown. $^{*}P < .05$ and $^{***}P < .001$.

wtSTAT3-expressing mice (see Fig E4, *E* and *F*). These data suggest that reactive astrocytes contribute to increases in GRP-evoked excitation of $GRPR^+$ SDH neurons under chronic itch conditions.

We reasoned that reactive astrocytes must signal $GRPR^+$ SDH neurons through secretion of biologically active signaling molecules. One potential candidate is LCN2, a factor released from astrocytes that has been implicated in patients with chronic itch.[9] In fact, expression of dnSTAT3 in astrocytes significantly suppressed *Lcn2* mRNA expression in the spinal cord because of DCP treatment (see Fig E2, *C*) in contrast to wtSTAT3 (see Fig E4, *G*).

To investigate the role of astrocytic LCN2 in the sensitization of $GRPR^+$ SDH neurons under chronic itch conditions, we used a CRISPR-Cas9–mediated *in vivo* gene-editing approach.[21] Because of the package size restriction of the AAV vector, we used *Staphylococcus aureus* Cas9 (SaCas9)[22] to produce an AAV-gfaABC$_1$D-SaCas9 vector (Fig 4, *A*), which enabled astrocyte-selective expression of SaCas9. The second AAV vector contained an *Lcn2*-targeting single-guide RNA expression cassette (sgLcn2, which was designed to cleave a site in exon 3 of the *Lcn2* gene; Fig 4, *B*) fused with gfaABC$_1$D-mCherry (AAV-gfaABC$_1$D-mCherry-U6-sgLcn2). AAV-gfaABC$_1$D-mCherry was used as a control (Fig 4, *A*). Immunohistochemical analysis revealed that SaCas9-expressing cells were immunostained with the astrocyte marker SOX9 (Fig 4, *C*).

To confirm astrocytic genome editing, we analyzed cleavage of the *Lcn2* genome in SDH astrocytes isolated by means of cell sorting with anti-astrocyte cell-surface antigen 2 (ACSA-2).[23] In addition to the band for the uncleaved *Lcn2* gene (Fig 4, *D*, arrow), we identified 2 bands at lower base pairs in SDH astrocytes obtained from mice expressing SaCas9 and sgLcn2 (Fig 4, *D*, arrowheads), indicating that the genome of astrocytic *Lcn2* had been edited. We observed no cleaved band for the astrocytic *Lcn2* gene in mice without sgLcn2 (Fig 4, *D*, and see Fig E5 in this article's Online Repository at www.jacionline.org). The editing efficiency in astrocytes of mice expressing sgLcn2 was statistically significant (Fig 4, *D*). In spinal cord slices obtained from DCP-treated sgLcn2 mice, we observed significant attenuation of GRP-induced increases in the depolarization of $GRPR^+$ neurons (Fig 4, *E* and *F*). Moreover, DCP-induced scratching behavior, skin lesioning, and skin barrier dysfunction were suppressed in these mice (Fig 4, *G-I*), indicating that LCN2 contributes to the sensitization of $GRPR^+$ SDH neurons, chronic itch, and dermatitis.

Finally, to determine whether LCN2 sufficiently enhances GRP-evoked excitation, we applied LCN2 to spinal slices obtained from normal *Grpr-EGFP* mice. In $GRPR^+$ neurons LCN2 had no effect on membrane potentials; however, coapplication of LCN2 and GRP (50 nmol/L) significantly enhanced GRP-induced depolarization (Fig 4, *J* and *K*). In addition, at a higher concentration of GRP (300 nmol/L), LCN2 enhanced depolarization in $GRPR^+$ neurons (see Fig E6 in this article's Online Repository at www.jacionline.org). These data indicate that LCN2 is sufficient to potentiate the GRP-induced excitability of $GRPR^+$ SDH neurons.

DISCUSSION

The present study is the first to demonstrate that GRP-induced excitability of $GRPR^+$ SDH neurons is enhanced under chronic itch conditions. Our immunohistochemical, electrophysiologic, and morphologic data indicated that more than half of $EGFP^+$ neurons in the SDH of *Grpr-EGFP* mice appeared to be vertical-type excitatory interneurons, which send excitatory signals to lamina I neurons that project to the brain.[12] Indeed, a recent study revealed that $GRPR^+$ neurons connect to lamina I projection neurons,[7] suggesting that enhancements in excitatory $GRPR^+$ signaling under chronic itch conditions are directly conveyed to lamina I projection neurons. Because the loss of $GRPR^+$ neurons markedly suppresses scratching behavior in a model of chronic itch associated with contact dermatitis,[6] the heightened sensitivity of $GRPR^+$ neurons to GRP might be an important neuronal alteration involved in the development of chronic itch.

We observed no alterations in *Grp* and *Grpr* mRNA expression in the spinal cords of DCP-treated mice, suggesting that increases in the excitability of $GRPR^+$ neurons are not simply due to their quantitative changes. Rather, we observed that suppression of reactive astrocytes through dnSTAT3 attenuated the excitability of $GRPR^+$ neurons in DCP mice, suggesting that reactive astrocytes are required to enhance GRP signaling in $GRPR^+$ neurons under chronic itch conditions. These findings are in accordance with the observed decrease in numbers of c-Fos^+ SDH neurons after astrocytic expression of dnSTAT3. Furthermore, by developing a method for enabling SDH astrocyte–specific gene editing in adult mice using the AAV-mediated CRISPR-Cas9 system, we demonstrated that LCN2 is crucial for the connection between SDH astrocytes and $GRPR^+$ neurons. LCN2 is produced and released from astrocytes,[9,24,25] which might presumably involve signals derived by IL-6[9] or IL-33,[26] and our findings indicate that LCN2 is sufficient to enhance the sensitivity of $GRPR^+$ SDH neurons to GRP. Thus the present study suggests that, under chronic itch conditions, sensitization of $GRPR^+$ neurons to GRP is associated with a non–cell-autonomous mechanism that involves reactive astrocytes and LCN2. On the other hand, the resting membrane potential of $GRPR^+$ neurons before GRP application was not altered in spinal cord slices taken from DCP-treated mice in which astrocytic LCN2 expression was upregulated. A possible explanation is that we used spinal cord slices with transected dorsal roots for patch-clamp recordings in $GRPR^+$ neurons, which implies that GRP-releasing neurons in the slices do not receive any excitatory inputs from the inflamed skin through primary afferents. Thus it is conceivable that a skin-derived pruritic signal to the SDH, which results in releasing GRP, might be needed for enhancing excitation of $GRPR^+$ neurons by LCN2. This view is supported by our data showing failure of LCN2 alone to depolarize $GRPR^+$ neurons.

SDH astrocyte–specific dnSTAT3 expression and *Lcn2* gene editing were also effective in treating dermatitis and skin barrier impairments. Because physical injury of the skin caused by scratching worsens dermatitis and skin barrier dysfunction, in turn increasing the itching sensation, our data suggest that SDH astrocyte–derived sensitization of $GRPR^+$ neurons through LCN2 is involved in the itch–scratch cycle that maintains chronic itch. In this study we revealed the sensitization of $GRPR^+$ SDH neurons by astrocytic LCN2 in the DCP model of contact dermatitis. However, skin barrier disruption caused by repetitive scratching also contributes to atopic dermatitis. We have previously found that activation of astrocytes and upregulation of LCN2 in the SDH are commonly observed in mouse models of contact and atopic dermatitis and that these are required for

chronic itch–related repetitive scratching behavior.[9] Therefore it is speculated that the facilitating effect of astrocytic LCN2 on itch neurotransmission in the SDH is also involved in repetitive scratching and the skin barrier disruption of atopic dermatitis. Thus the implications of our findings obtained from the DCP model of contact dermatitis would provide valuable information for considering the mechanism underlying chronic itch and skin barrier dysfunction associated with atopic dermatitis.

The mechanism underlying the LCN2-mediated sensitization of $GRPR^+$ neurons remains to be determined. We observed no effect of astrocytic dnSTAT3 on *Grpr* mRNA expression in the spinal cord, suggesting that activated astrocytes functionally modulate GRPR signaling. However, we cannot rule out the possibility that astrocytes change GRPRs at posttranscriptional levels (eg, protein levels of GRPR or its translocation to the plasma membrane).

Within the brain, LCN2 has been reported to modulate neuronal morphology, synaptic plasticity,[27,28] neuronal death,[24] and neuronal excitability.[29] Previous research has also identified SLC22A17,[30] megaline,[31] and melanocortin 4 receptor[29] as candidate receptors for LCN2. However, the receptors responsible for LCN2-induced sensitization of $GRPR^+$ neurons in patients with chronic itch remain to be determined. Given that coapplication of LCN2 and GRP enhanced the GRP response in the present study, we speculate that LCN2 acutely enhances the sensitivity of $GRPR^+$ neurons to GRP. Melanocortin 4 receptor, which enables activation of intracellular protein kinase A through G_s proteins,[29] appears to be a candidate for mediating the acute biological effects of LCN2. Furthermore, a recent study has reported that excitation of $GRPR^+$ neurons by GRP involves an inhibition of Kv4 channels, members of the family of voltage-gated K^+ channels,[32] but we found that LCN2 had no effect on A-type K^+ current (see Fig E7 in this article's Online Repository at www.jacionline.org), which is mainly mediated by Kv4 channels.[33] Because LCN2 has been also shown to be involved in patients with other neuroinflammatory diseases, including Parkinson disease,[34] amyotrophic lateral sclerosis,[35] and brain injury,[36] further studies are required to identify the LCN2 receptors that modulate neuronal activity.

In the present study we analyzed $GRPR^+$ neurons identified as excitatory through electrophysiologic and immunohistochemical experiments. However, GRP-induced excitation in $GRPR^+$ neurons seems not to be uniform because $EGFP^+$ neurons exhibiting a delayed firing pattern were more sensitive to GRP. Furthermore, approximately 20% of total $GRPR^+$ neurons were inhibitory. It is conceivable that the groups of $GRPR^+$ neurons with each firing pattern might have a distinct role in itch transmission, but this remains unclear and needs further investigation.

Although the CRISPR-Cas9 system is an efficient and widely used genome-editing tool,[21] spatiotemporally controlled editing is difficult using this system. AAV vectors are useful for introducing certain genes, but *Streptococcus pyogenes* Cas9 is too large for AAV vectors. However, recent studies have led to the development of an efficient and target-specific *in vivo* genome-editing technique that relies on SaCas9, a small Cas9 derived from *Staphylococcus aureus*.[22,37] In the present study we used SaCas9 and the astrocyte-specific promoter $gfaABC_1D$, demonstrating AAV-mediated editing of the astrocytic *Lcn2* gene. The editing efficiency was approximately 20%, which was similar to or slightly lower than that reported in previous studies.[37] Nonetheless, efficiency might have been underestimated in our study because we analyzed SDH astrocytes sorted using ACSA-2, an antibody that marks all astrocytes with or without expression of SaCas9, sgLcn2, or both. Alternatively, because we used 2 AAV vectors containing either SaCas9 or sgLcn2 for CRISPR-Cas9–mediated genome editing, the number of SDH astrocytes infected with both viruses might have been low.

Despite these limitations, we achieved cleavage of the *Lcn2* genome in adult mice *in vivo*, which significantly influenced the hyperexcitability of $GPRP^+$ SDH neurons, chronic itch symptoms, and dermatitis. Therefore this approach might be useful for investigating the functions of astrocytes under physiologic and pathologic conditions.

In conclusion, our findings demonstrate that GRP-evoked excitation in $GRPR^+$ SDH neurons is potentiated in a mouse model of chronic itch, without concomitant changes in GRPR expression in the SDH. Potentiation of GRP-induced neuronal excitation was attenuated by suppressing the reactive state of SDH astrocytes and by astrocyte-selective editing of the *Lcn2* gene using the AAV–CRISPR-Cas9 system. Moreover, our findings indicated that LCN2 is sufficient for potentiating GRP-induced excitation of $GRPR^+$ neurons in normal mice. Therefore our results suggest that, under chronic itch conditions, the excitatory response of $GRPR^+$ neurons to GRP is sensitized through a non–cell-autonomous mechanism involving LCN2 derived from reactive astrocytes. In primates GRP-GRPR signaling in the SDH are also involved in itch transmission.[38] If SDH astrocytes are activated and produce LCN2 in patients with chronic itch (which needs future research), reactive astrocytes and LCN2 might represent a therapeutic target for alleviating spinal sensitization of itch transmission neurons and chronic itch.

We thank the University of Pennsylvania vector core for providing pZac2.1, pAAV2/9, and pAdDeltaF6 plasmid. We would like to thank Editage (www.editage.jp) for English-language editing.

Key messages

- **GRP-GRPR signaling was potentiated in SDH neurons from mice with contact dermatitis.**
- **Genetic inhibition of reactive SDH astrocytes and CRISPR-Cas9–mediated editing of the astrocytic *Lcn2* gene prevented increases in GRP-GRPR signaling, chronic itch, and dermatitis.**

REFERENCES

1. Ikoma A, Steinhoff M, Stander S, Yosipovitch G, Schmelz M. The neurobiology of itch. Nat Rev Neurosci 2006;7:535-47.
2. Koch SC, Acton D, Goulding M. Spinal circuits for touch, pain, and itch. Annu Rev Physiol 2018;80:189-217.
3. Yosipovitch G, Rosen JD, Hashimoto T. Itch: from mechanism to (novel) therapeutic approaches. J Allergy Clin Immunol 2018;142:1375-90.
4. Dong X, Dong X. Peripheral and central mechanisms of itch. Neuron 2018;98:482-94.
5. Sun YG, Chen ZF. A gastrin-releasing peptide receptor mediates the itch sensation in the spinal cord. Nature 2007;448:700-3.
6. Sun YG, Zhao ZQ, Meng XL, Yin J, Liu XY, Chen ZF. Cellular basis of itch sensation. Science 2009;325:1531-4.
7. Mu D, Deng J, Liu KF, Wu ZY, Shi YF, Guo WM, et al. A central neural circuit for itch sensation. Science 2017;357:695-9.
8. Zhao ZQ, Huo FQ, Jeffry J, Hampton L, Demehri S, Kim S, et al. Chronic itch development in sensory neurons requires BRAF signaling pathways. J Clin Invest 2013;123:4769-80.

9. Shiratori-Hayashi M, Koga K, Tozaki-Saitoh H, Kohro Y, Toyonaga H, Yamaguchi C, et al. STAT3-dependent reactive astrogliosis in the spinal dorsal horn underlies chronic itch. Nat Med 2015;21:927-31.
10. Zhao ZQ, Liu XY, Jeffry J, Karunarathne WK, Li JL, Munanairi A, et al. Descending control of itch transmission by the serotonergic system via 5-HT1A-facilitated GRP-GRPR signaling. Neuron 2014;84:821-34.
11. Yasaka T, Tiong SY, Hughes DI, Riddell JS, Todd AJ. Populations of inhibitory and excitatory interneurons in lamina II of the adult rat spinal dorsal horn revealed by a combined electrophysiological and anatomical approach. Pain 2010; 151:475-88.
12. Lu Y, Perl ER. Modular organization of excitatory circuits between neurons of the spinal superficial dorsal horn (laminae I and II). J Neurosci 2005;25:3900-7.
13. Koga K, Kanehisa K, Kohro Y, Shiratori-Hayashi M, Tozaki-Saitoh H, Inoue K, et al. Chemogenetic silencing of GABAergic dorsal horn interneurons induces morphine-resistant spontaneous nocifensive behaviours. Sci Rep 2017;7: 4739.
14. Cheng L, Samad OA, Xu Y, Mizuguchi R, Luo P, Shirasawa S, et al. Lbx1 and Tlx3 are opposing switches in determining GABAergic versus glutamatergic transmitter phenotypes. Nat Neurosci 2005;8:1510-5.
15. van der Steen PH, van Baar HM, Perret CM, Happle R. Treatment of alopecia areata with diphenylcyclopropenone. J Am Acad Dermatol 1991;24:253-7.
16. Mishra SK, Hoon MA. The cells and circuitry for itch responses in mice. Science 2013;340:968-71.
17. Sofroniew MV. Molecular dissection of reactive astrogliosis and glial scar formation. Trends Neurosci 2009;32:638-47.
18. Kohro Y, Sakaguchi E, Tashima R, Tozaki-Saitoh H, Okano H, Inoue K, et al. A new minimally-invasive method for microinjection into the mouse spinal dorsal horn. Sci Rep 2015;5:14306.
19. Kanehisa K, Shiratori-Hayashi M, Koga K, Tozaki-Saitoh H, Kohro Y, Takamori K, et al. Specific activation of inhibitory interneurons in the spinal dorsal horn suppresses repetitive scratching in mouse models of chronic itch. J Dermatol Sci 2017;88:251-4.
20. Bonni A, Sun Y, Nadal-Vicens M, Bhatt A, Frank DA, Rozovsky I, et al. Regulation of gliogenesis in the central nervous system by the JAK-STAT signaling pathway. Science 1997;278:477-83.
21. Heidenreich M, Zhang F. Applications of CRISPR-Cas systems in neuroscience. Nat Rev Neurosci 2016;17:36-44.
22. Ran FA, Cong L, Yan WX, Scott DA, Gootenberg JS, Kriz AJ, et al. In vivo genome editing using *Staphylococcus aureus* Cas9. Nature 2015;520: 186-91.
23. Swartzlander DB, Propson NE, Roy ER, Saito T, Saido T, Wang B, et al. Concurrent cell type-specific isolation and profiling of mouse brains in inflammation and Alzheimer's disease. JCI Insight 2018;3.
24. Bi F, Huang C, Tong J, Qiu G, Huang B, Wu Q, et al. Reactive astrocytes secrete lcn2 to promote neuron death. Proc Natl Acad Sci U S A 2013;110:4069-74.
25. Suk K. Lipocalin-2 as a therapeutic target for brain injury: an astrocentric perspective. Prog Neurobiol 2016;144:158-72.
26. Du L, Hu X, Yang W, Yasheng H, Liu S, Zhang W, et al. Spinal IL-33/ST2 signaling mediates chronic itch in mice through the astrocytic JAK2-STAT3 cascade. Glia 2019;67:1680-93.
27. Ferreira AC, Pinto V, Da Mesquita S, Novais A, Sousa JC, Correia-Neves M, et al. Lipocalin-2 is involved in emotional behaviors and cognitive function. Front Cell Neurosci 2013;7:122.
28. Mucha M, Skrzypiec AE, Schiavon E, Attwood BK, Kucerova E, Pawlak R. Lipocalin-2 controls neuronal excitability and anxiety by regulating dendritic spine formation and maturation. Proc Natl Acad Sci U S A 2011;108:18436-41.
29. Mosialou I, Shikhel S, Liu JM, Maurizi A, Luo N, He Z, et al. MC4R-dependent suppression of appetite by bone-derived lipocalin 2. Nature 2017;543:385-90.
30. Devireddy LR, Gazin C, Zhu X, Green MR. A cell-surface receptor for lipocalin 24p3 selectively mediates apoptosis and iron uptake. Cell 2005;123:1293-305.
31. Hvidberg V, Jacobsen C, Strong RK, Cowland JB, Moestrup SK, Borregaard N. The endocytic receptor megalin binds the iron transporting neutrophil-gelatinase-associated lipocalin with high affinity and mediates its cellular uptake. FEBS Lett 2005;579:773-7.
32. Pagani M, Albisetti GW, Sivakumar N, Wildner H, Santello M, Johannssen HC, et al. How gastrin-releasing peptide opens the spinal gate for itch. Neuron 2019; 103:102-117, e5.
33. Hu HJ, Carrasquillo Y, Karim F, Jung WE, Nerbonne JM, Schwarz TL, et al. The kv4.2 potassium channel subunit is required for pain plasticity. Neuron 2006;50: 89-100.
34. Kim BW, Jeong KH, Kim JH, Jin M, Kim JH, Lee MG, et al. Pathogenic upregulation of glial lipocalin-2 in the Parkinsonian dopaminergic system. J Neurosci 2016;36:5608-22.
35. Tong J, Huang C, Bi F, Wu Q, Huang B, Liu X, et al. Expression of ALS-linked TDP-43 mutant in astrocytes causes non-cell-autonomous motor neuron death in rats. EMBO J 2013;32:1917-26.
36. Jin M, Kim JH, Jang E, Lee YM, Soo Han H, Woo DK, et al. Lipocalin-2 deficiency attenuates neuroinflammation and brain injury after transient middle cerebral artery occlusion in mice. J Cereb Blood Flow Metab 2014;34:1306-14.
37. Kumar N, Stanford W, de Solis C, Aradhana, Abraham ND, Dao TJ, et al. The development of an AAV-based CRISPR SaCas9 genome editing system that can be delivered to neurons in vivo and regulated via doxycycline and Cre-recombinase. Front Mol Neurosci 2018;11:413.
38. Lee H, Ko MC. Distinct functions of opioid-related peptides and gastrin-releasing peptide in regulating itch and pain in the spinal cord of primates. Sci Rep 2015;5: 11676.

METHODS

Animals

Male *Grpr-EGFP* mice (STOCK Tg[Grpr-EGFP]PZ62Gsat/Mmucd; Mutant Mouse Resource and Research Center) and wild-type ICR mice (CLEA) were used. All mice used were aged 8 to 12 weeks at the start of each experiment and housed individually and in groups of 2 or 3 per cage at a temperature of 22°C ± 1°C with a 12-hour light-dark cycle (light on 8 AM to 8 PM) and were fed food and water *ad libitum*. All animal experiments were conducted according to relevant national and international guidelines contained in the Act on Welfare and Management of Animals (Ministry of Environment of Japan) and Regulation of Laboratory Animals (Kyushu University) and under protocols approved by the Institutional Animal Care and Use committee review panels at Kyushu University.

Recombinant AAV vector production

We constructed plasmids (gfaABC$_1$D-mCherry, gfaABC$_1$D-dnSTAT3, or gfaABC$_1$D-wtSTAT3) from the cis-cloning plasmid pZac2.1.[E1] Genes encoding U6-sgRNA (plasmid #61593; Addgene, Cambridge, Mass)[E2] and SaCsa9 (plasmid #78601; Addgene)[E3] were subcloned into the pENTR plasmid. Synthetic oligonucleotides included the targeting sequence for *Lcn2* (5′-GCCAGGACCAGGGCTGTCGCTA-3′) with the targeting site in the original pENTER-U6-sgBsa1 plasmid. The resulting U6-sgRNA cassette was transferred into pZac2.1-gfaABC$_1$D-mCherry plasmid. The SaCas9 cassette was transferred into the AAV shuttle vector with gfaABC$_1$D (pZac2.1-gfaABC$_1$D-saCas9). Recombinant AAV vectors were produced from HEK293 cells with triple transfection (each pZac2.1 plasmid, pAAV2/5 [transfer plasmid], and pAdDeltaF6 [adenoviral helper plasmid]; the latter 2 plasmids were purchased from the University of Pennsylvania Gene Therapy Program Vector Core). Viral lysates were harvested at 72 hours after transfection and lysed by using freeze-and-thaw cycles, purified through 2 rounds of CsCl ultracentrifugation, and then concentrated with Vivaspin 20 ultrafiltration units (SARSTEDT, Nümbrecht, Germany). The genomic titer of recombinant AAV was determined by using PicoGreen fluorometric reagent (Molecular Probes, Eugene, Ore) after denaturation of the AAV particle. Vectors were stored in aliquots at −80°C until use.

Microinjection of recombinant AAV into the cervical SDH

Mice were deeply anesthetized by means of subcutaneous injection of ketamine (100 mg/kg) and xylazine (10 mg/kg). Mice were shaved on the back of the neck, and skin was incised at the C3-C5 vertebrae. The muscle on the C3-C5 vertebrae was opened with a retractor, and mice were attached to a head-holding device (SR-AR; NARISHIGE, Setagaya City, Japan). Paraspinal muscles around the left side of the interspace between the C3 and C4 vertebrae were removed, and the dura mater and arachnoid membrane were carefully incised by using the tip of a 30-gauge needle to make a small window to allow a glass microcapillary insert directly into the SDH. The glass microcapillary was inserted into the SDH (150-200 μm in depth from the surface of the dorsal root entry zone) with a preflow of recombinant AAV solution through the small window (approximately 500 μm lateral from the midline). Recombinant AAV solution was pressure ejected (100 nL/min) for 5 minutes (approximately 500 nL) with Micro Syringe Pumps. After microinjection, the inserted glass microcapillary was removed from the SDH, the skin was sutured with 3-0 silk, and mice were kept under a heating light until recovery.

Immunohistochemistry

As we previously reported,[E4] mice were deeply anesthetized by means of intraperitoneal injection of pentobarbital (100 mg/kg) and perfused transcardially with 20 mL of PBS (WAKO, Saitama, Japan), followed by 50 mL of ice-cold 4% paraformaldehyde/PBS. The C3 to C5 segments of the spinal cord were removed, postfixed in the same fixative for 3 hours at 4°C, and placed in 30% sucrose solution for 48 hours at 4°C. Transverse spinal cord (30 μm) sections were incubated in blocking solution (3% normal goat serum) for 2 hours at room temperature and then incubated for 48 hours at 4°C with primary antibodies, mouse anti–neuronal nuclei (1:2000; ab104224, Abcam, Cambridge, United Kingdom), goat anti–paired box 2 (1:1000; AF3075; R&D Systems, Minneapolis, Minn), rabbit anti-GFP (1:500; #598; MBL, Nagoya, Japan), isolectin GS–isolectin B4 biotin conjugate (1:1000; 121414, Thermo Fisher, Waltham, Mass), and rabbit anti–c-Fos (1:1000; 9F6; Cell Signaling, Danvers, Mass). After incubation, tissue sections were washed and incubated for 3 hours at room temperature in secondary antibody solution (Alexa Fluor 488, 546, and/or 405; Molecular Probes). Tissue sections were washed, slide mounted, and subsequently placed under coverslips with VECTASHIELD Hardmount (Vector Laboratories, Burlingame, Calif). Immunofluorescence images were obtained with a confocal laser microscope (LSM700; Carl Zeiss, Oberkochen, Germany). Fluorescence intensity was quantified with ImageJ software (National Institutes of Health, Bethesda, Md). Numbers of c-Fos$^+$ cells in the superficial dorsal horn (lamina I–IIo), which were identified by using isolectin B4 staining, were counted.

Electrophysiology

Mice were deeply anesthetized with ketamine (100 mg/kg) and xylazine (10 mg/kg), and the cervical spinal cord was removed and placed in a cold high-sucrose artificial cerebrospinal fluid (sucrose aCSF; 250 mmol/L sucrose, 2.5 mmol/L KCl, 2 mmol/L $CaCl_2$, 2 mmol/L $MgCl_2$, 1.2 mmol/L NaH_2PO_4, 25 mmol/L $NaHCO_3$, and 11 mmol/L glucose). A parasagittal spinal cord slice (250-300 μm thick) was made with a vibrating microtome (VT1200; Leica, Wetzlar, Germany), and then the slices were kept in oxygenated aCSF solution (125 mmol/L NaCl, 2.5 mmol/L KCl, 2 mmol/L $CaCl_2$, 1 mmol/L $MgCl_2$, 1.25 mmol/L NaH_2PO_4, 26 mmol/L $NaHCO_3$, and 20 mmol/L glucose) at room temperature (22°C-25°C) for at least 30 minutes. The spinal cord slice was then put into a recording chamber, where it was continuously superfused with aCSF solution at 25°C to 28°C at a flow rate of 4 to 6 mL/min. Patch pipettes were filled with an internal solution (125 mmol/L K-gluconate, 10 mmol/L KCl, 0.5 mmol/L EGTA, 10 mmol/L HEPES, 4 mmol/L ATP-Mg, 0.3 mmol/L NaGTP, 10 mmol/L phosphocreatine, and 0.4% neurobiotin [pH 7.28] adjusted with KOH), and whole-cell patch-clamp recordings were made from EGFP$^+$ SDH neurons. Recordings were made with the Axopatch 700B amplifier and pCLAMP 10.4 acquisition software (Molecular Devices). Data were digitized with an analog-to-digital converter (Digidata 1550; Molecular Devices), stored on a personal computer with a data acquisition program (ClampeX version 10.4; Molecular Devices), and analyzed with a software package (Clampfit version 10.4; Molecular Devices). Membrane potentials were recorded in current-clamp mode. All drugs were dissolved in aCSF solution and superfused for 2 minutes. The drugs used were GRP (50 or 300 nmol/L; Bachem, Bubendorf, Switzerland) and LCN2 (10 nmol/L; R&D Systems). We quantified averaged membrane potential for 30 seconds of predrug and postdrug application. The amplitude of the A-type K$^+$ current was measured by subtracting the steady-state current during 200 to 250 ms of voltage pulse from the maximal current evoked by the voltage step from –80 to –30 mV. The firing patterns of neurons were determined in current-clamp mode by passing depolarizing current pulses for 1 second through the recording electrode from the resting membrane potential.[E5]

Classification criteria of morphology of SDH neurons

Criteria of neuronal morphology were based on previous literature.[E6] Central cells have dendritic arbors distributed principally rostrocaudally for 150 to 275 μm, with only small dorsoventral extensions. Vertical cells have dendrites extensively distributed dorsoventrally for 150 to 200 μm, as well as rostrocaudally. Radial cells have dendrites that extend in several directions in the parasagittal plane.

Mouse model of chronic itch

DCP (Wako) dissolved in acetone was used to induce contact dermatitis. Mice were shaved on the back and topically applied by painting 0.2 mL of

DCP (1% for wild-type ICR mice and 2% for *Grpr-EGFP* mice) on the back skin after achivement of isoflurane anesthesia. Seven days after the first painting, DCP was painted again on the same area of skin.

Measurement of TEWL

TEWL was measured with the Tewameter TM300 system and a multiprobe adaptor (CK Electronic, Köln, Germany) in accordance with the manufacturer's instructions. After achievement of isoflurane anesthesia, the probe collar was placed on the surface of the skin on the animal's back for 20 to 30 seconds. Measurements were obtained twice for the left and right sides of the skin, and values were averaged.

Real-time RT-PCR

As we previously reported,[E4] mice were anesthetized with pentobarbital and perfused transcardially with PBS. The C3-C5 segments of the spinal cord were removed immediately. Total RNA was extracted with TRIsure (Bioline, London, United Kingdom), according to the manufacturer's protocol. The amount of total RNA was quantified by measuring OD at 260 nm (OD260) with a spectrophotometer (Nanodrop One; Thermo Fisher). For reverse transcription, 250 ng of total RNA was transferred to the reaction with PrimeScript Reverse Transcriptase (Takara, Shiga, Japan) and random 6-mer primers. Quantitative PCR was carried out with FastStart Essential DNA Probes Master or FastStart Essential DNA Green Master (Roche, Basel, Switzerland) using the LightCycler 96 (Roche), according to the manufacturer's specifications, and data were analyzed by using LightCycler 96 Software (Roche) with standard curves. Values were normalized to *Actb* expression. The TaqMan probe, forward primer, and reverse primer used in this study were as follows: *Lcn2*, forward primer 5′-CCCCATCTCTGCTC ACTGTC-3′ and reverse primer 5′-TTTTTCTGGACCGCATTG-3′; *Actb*, probe 5′-FAM-CCTGGCCTCACTGTCCACCTTCCA-TAMRA-3′, forward primer 5′-CCTGAGCGCAAGTACTCTGTGT-3′, and reverse primer 5′-CTGCTTGCTGATCCACATCTG-3′; *Nppb*, probe 5′-FAM-CTGCTTTTCC TTTATCTGTCACCGCTGG-TAMRA-3′, forward primer 5′-GTGCTGTCC CAGATGATTCTGTT-3′, and reverse primer 5′-CTCCAGCAGCTTCTGC ATCTT -3′; and *Grp*, probe 5′-FAM-CCCGAGGACGGCAGCTACTTT AACGA-TAMRA-3′, forward primer 5′-GAAGCTGCTGGGAACCAAAG-3′, and reverse primer 5′-GGAGCAGAGAGTCTACCAACTTAGC-3′. For *Grpr* mRNA, validated probe and primers (Mm01157247_m1; Applied Biosystems, Foster City, Calif) were used.

Measurement of scratching behavior

Scratching behavior in mice was automatically detected and objectively evaluated by using MicroAct (Neuroscience) in accordance with a previously described method.[E4] Briefly, after achievement of isoflurane anesthesia, a small Teflon-coated magnet (1 mm in diameter and 3 mm in length; Neuroscience) was implanted subcutaneously into the hind paws of the mice at least 1 day before the first recording. Each mouse with an implanted magnet was placed in an observation chamber (11 cm in diameter and 18 cm high) with food and tap water surrounded by a round coil. Movement of magnets implanted subcutaneously into the hind paws induced electric currents in the coil, which were amplified and recorded by using MicroAct software. Analytic parameters for detecting scratch movements were as follows: threshold, 0.07 V; event gap, 0.2 seconds; minimum duration, 0.2 seconds; maximum frequency, 35 Hz; minimum frequency, 2 Hz; and minimum beats, 2. Scratching behavior was shown as the number of total scratching strokes over 24 hours.

Dissociation of SDH tissue and cell sorting

Mice were perfused with ice-cold Hanks balanced salt solution (HBSS[–]), after which C3-C5 of the SDH were dissected, gently minced with sterile razorblades, and suspended in HBSS(–) with activated papain (20 U of LK003172; Worthington Biochemical, Lakewood, NJ) and 0.2 mg of L-cysteine. Suspended SDH tissue was incubated for 20 minutes at 34°C and treated with DNase and $MgCl_2$ for 5 minutes. Then ice-cold HBSS(–) with 4 mmol/L EDTA and 0.5% BSA was added to the suspension, which was centrifuged at 300*g* for 5 minutes at 4°C. The pellet was resuspended and gently triturated with an 18-gauge needle. The cell suspension was kept on ice for 1 to 2 minutes to allow the larger tissue to settle, and the supernatant was carefully transferred to a tube. HBSS(–) with 1% FBS was added to the original tube, and the process was repeated with 23- and 26-gauge needles. The supernatant was added to the 1- mL tube, filtered through a 70-μm cell strainer, and centrifuged. Myelin Removal Beads II (Miltenyi Biotec, Bergisch Gladbach, Germany), and columns (Miltenyi Biotec) were used to remove myelin debris in accordance with the manufacturer's protocol. The resulting flowthrough was centrifuged at 300*g* for 10 minutes at 4°C. The pellet was resuspended with blocking buffer (1:100; BD Biosciences, San Jose, Calif) for 5 minutes.

For cell type labeling, the suspension was incubated with anti-CD11b–Alexa Fluor 647 (1:1000; BD Biosciences) and ACSA-2–fluorescein isothiocyanate (1:200; Miltenyi Biotec).[E7] After incubation, the suspension was washed and centrifuged at 300*g* for 10 minutes at 4°C. Cells were resuspended and filtered through a 40-μm cell strainer. Fluorescence-activated cell sorting was performed with the BD FACSAria III (BD Biosciences). Cells were sorted into 15-mL tubes containing 1% FBS, after which they were again centrifuged and resuspended for DNA extraction.

DNA extraction and assessment of *in vivo* genome editing

DNA was extracted from the sorted astrocytes by using a Quick-DNA Microprep kit (Zymo Research, Irvine, Calif) in accordance with the manufacturer's protocol. The region containing the sgRNA target site was PCR amplified from genomic DNA by using specially designed primers (sgLcn2 forward: AAAGGTCTTAGCAGGACCAG, sgLcn2 reverse: GAGACTGGGGTGTAACCTG). The resultant PCR-amplified DNA was evaluated by using a resolvase-based mutation detection kit (Clontech, Mountain View, Calif). Briefly, DNA was amplified with a Phusion High-Fidelity PCR Kit (Thermo Fisher), and DNA hybridization was performed with 10 μL of PCR products, followed by incubation with resolvase. The digested products were electrophoresed on a 1.5% agarose 1 × TBE gel, and the amount of editing was quantified with ImageJ software. Editing efficiency was defined as the average value of cleaved DNA fragments compared with the total amount of DNA (uncleaved and cleaved DNA fragments).[E8,E9]

Statistical analysis

All data are shown as means ± SEMs. Statistical significance of differences was determined by using the paired *t* test (Fig E7, *B*), the unpaired *t* test (Fig 2, *E* and *F*; Fig 3, *F*; Fig 4, *F*; Fig E1, *A-C*; Fig E2, *A*; Fig E2, *B*; Fig E3, *A*; Fig E4, *B*, *C*, *F*, and *G*; and Fig E6, *B*), the unpaired *t* test with the Welch correction (Fig E2, *C*), the Mann-Whitney test (Fig 2, *C*; Fig 3, *G* and *J*; Fig 4, *D* and *I*; Fig E3, *C*, and Fig E4, *E*), 2-way repeated-measures ANOVA with the post hoc Bonferroni test (Fig 2, *A*; Fig 3, *H*; Fig 4, *G*; Fig E3, *B*, and Fig E4, *D*), and 1-way ANOVA with the *post hoc* Tukey multiple comparisons test (Fig 3, *D*, and Fig 4, *K*) by using GraphPad Prism 4 and 7 software (GraphPad Software, La Jolla, Calif). Differences were considered significant at a *P* value of less than .05.

REFERENCES

E1. Kohro Y, Sakaguchi E, Tashima R, Tozaki-Saitoh H, Okano H, Inoue K, et al. A new minimally-invasive method for microinjection into the mouse spinal dorsal horn. Sci Rep 2015;5:14306.

E2. Ran FA, Cong L, Yan WX, Scott DA, Gootenberg JS, Kriz AJ, et al. In vivo genome editing using *Staphylococcus aureus* Cas9. Nature 2015;520:186-91.

E3. Tabebordbar M, Zhu K, Cheng JKW, Chew WL, Widrick JJ, Yan WX, et al. In vivo gene editing in dystrophic mouse muscle and muscle stem cells. Science 2016;351:407-11.

E4. Shiratori-Hayashi M, Koga K, Tozaki-Saitoh H, Kohro Y, Toyonaga H, Yamaguchi C, et al. STAT3-dependent reactive astrogliosis in the spinal dorsal horn underlies chronic itch. Nat Med 2015;21:927-31.

E5. Koga K, Kanehisa K, Kohro Y, Shiratori-Hayashi M, Tozaki-Saitoh H, Inoue K, et al. Chemogenetic silencing of GABAergic dorsal horn interneurons induces morphine-resistant spontaneous nocifensive behaviours. Sci Rep 2017;7:4739.

E6. Yasaka T, Tiong SY, Hughes DI, Riddell JS, Todd AJ. Populations of inhibitory and excitatory interneurons in lamina II of the adult rat spinal dorsal horn revealed by a combined electrophysiological and anatomical approach. Pain 2010;151:475-88.

E7. Swartzlander DB, Propson NE, Roy ER, Saito T, Saido T, Wang B, et al. Concurrent cell type-specific isolation and profiling of mouse brains in inflammation and Alzheimer's disease. JCI Insight 2018;3.

E8. Vouillot L, Thelie A, Pollet N. Comparison of T7E1 and surveyor mismatch cleavage assays to detect mutations triggered by engineered nucleases. G3 (Bethesda) 2015;5:407-15.

E9. Kumar N, Stanford W, de Solis C, Aradhana, Abraham ND, Dao TJ, et al. The development of an AAV-based CRISPR SaCas9 genome editing system that can be delivered to neurons in vivo and regulated via doxycycline and Cre-recombinase. Front Mol Neurosci 2018;11:413.

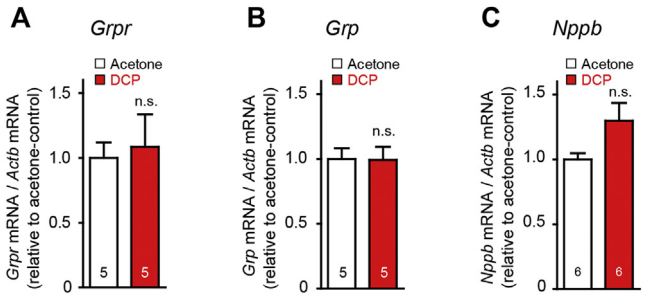

FIG E1. mRNA expression in the spinal cords and dorsal root ganglia of acetone- and DCP-treated mice. **A** and **B,** *Grpr* and *Grp* mRNA expression in the spinal cord (C3-C5) of acetone- and DCP-treated mice at day 14 from the first treatment (acetone, n = 5; DCP, n = 5). **C,** *Nppb* mRNA expression in the dorsal root ganglia (C3-C5) of acetone- and DCP-treated mice at day 14 from the first treatment (acetone, n = 5; DCP, n = 5). Values represent ratios of mRNA (normalized to *Actb* mRNA value) to the value of acetone-treated mice. Data are shown as means ± SEMs. *n.s.*, Not significant.

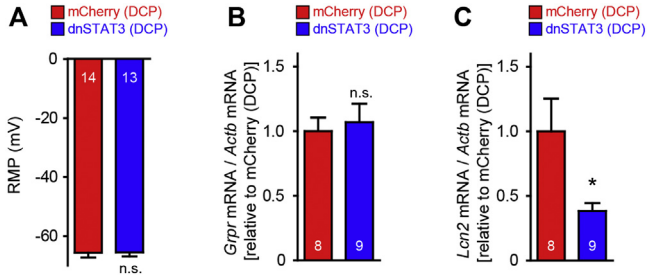

FIG E2. Comparisons between astrocytic mCherry- and dnSTAT-expressing DCP-treated mice. **A,** Resting membrane potential *(RMP)* of $GRPR^{+}$ neurons in the SDH of DCP-treated mCherry and dnSTAT mice (mCherry [DCP], n = 14; dnSTAT [DCP], n = 13). **B,** *Grpr* mRNA expression in the spinal cords of DCP-treated mice with astrocytic mCherry or dnSTAT expression at day 14 from first DCP treatment (mCherry [DCP], n = 8; dnSTAT [DCP], n = 9). **C,** *Lcn2* mRNA expression in the spinal cords of DCP-treated mice with astrocytic mCherry or dnSTAT expression at day 14 from the first DCP treatment (mCherry [DCP], n = 8; dnSTAT [DCP], n = 9). **P* < .05. Data are shown as means ± SEMs. *n.s.*, Not significant.

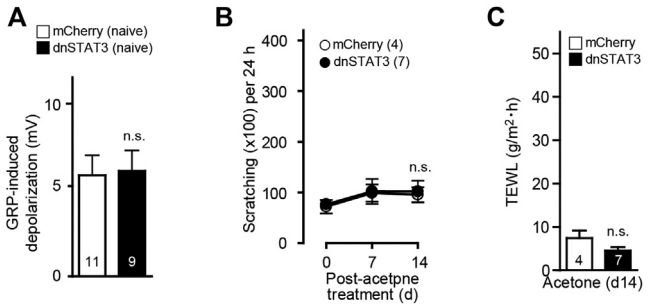

FIG E3. Comparisons between astrocytic mCherry- and dnSTAT-expressing mice. **A,** GRP-induced depolarization of $GRPR^{+}$ neurons in the SDH of naive mice with astrocytic expression of mCherry or dnSTAT mice (mCherry [naive], n = 11; dnSTAT [naive], n = 9). **B** and **C,** Effects of dnSTAT3 on scratching behavior (Fig E3, *B*) and TEWL (Fig E3, *C*) in acetone-treated mice (Fig E3, *B*: mCherry, n = 4; dnSTAT3, n = 7; Fig E3, *C*: mCherry, n = 4; dnSTAT3, n = 7). Data are shown as means ± SEMs. *n.s.*, Not significant.

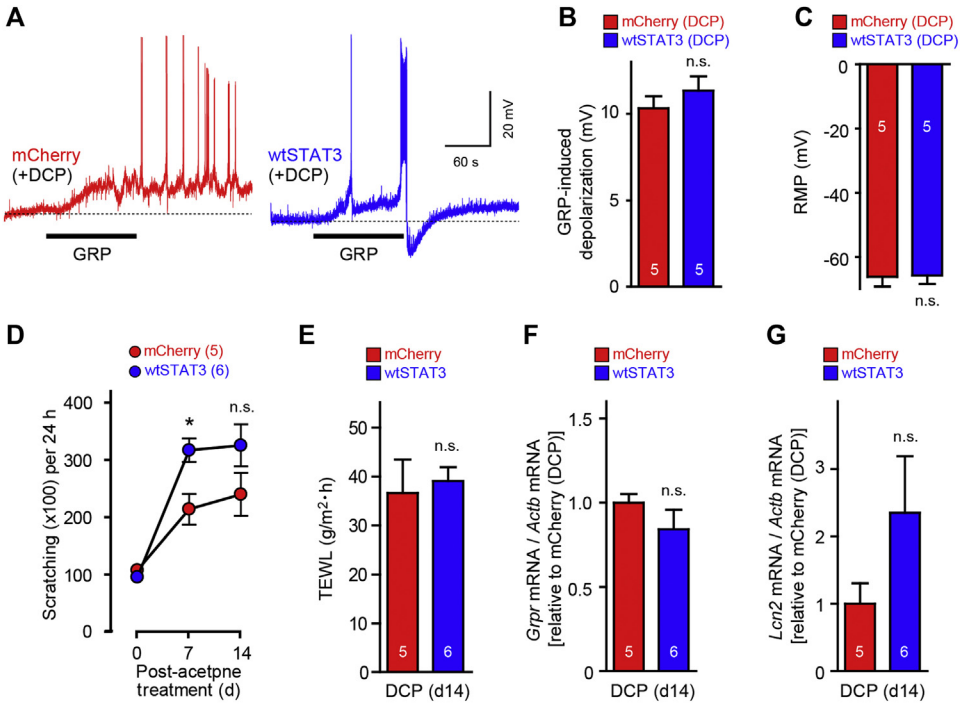

FIG E4. Astrocytic wtSTAT3 expression in DCP-treated mice. **A** and **B,** GRP-induced depolarization of $GRPR^{+}$ SDH neurons in DCP-treated *Grpr-EGFP* mice with AAV-mCherry or wtSTAT3 at days 13 or 14. Representative traces (Fig E4, *A*) and averaged data [Fig E4, *B*; mCherry [DCP], n = 5; wtSTAT3 [DCP], n = 5). **C,** RMP of $GRPR^{+}$ neurons in the SDH of DCP-treated mCherry and wtSTAT3 mice (mCherry [DCP], n = 5; wtSTAT3 [DCP], n = 5). **D** and **E,** Effect of wtSTAT3 on scratching behavior (Fig E4, *D*: mCherry [DCP], n = 5; wtSTAT3 [DCP], n = 6; $*P < .05$) and TEWL in DCP-treated mice (Fig E4, *E*: mCherry [DCP], n = 5; wtSTAT3 [DCP], n = 6). **F** and **G,** *Grpr* and *Lcn2* mRNA expression in the spinal cords of DCP-treated mCherry and wtSTAT3 mice at day 14 from the first DCP treatment (mCherry [DCP], n = 5; wtSTAT3 [DCP], n = 6). Data are shown as means ± SEMs. *n.s.*, Not significant.

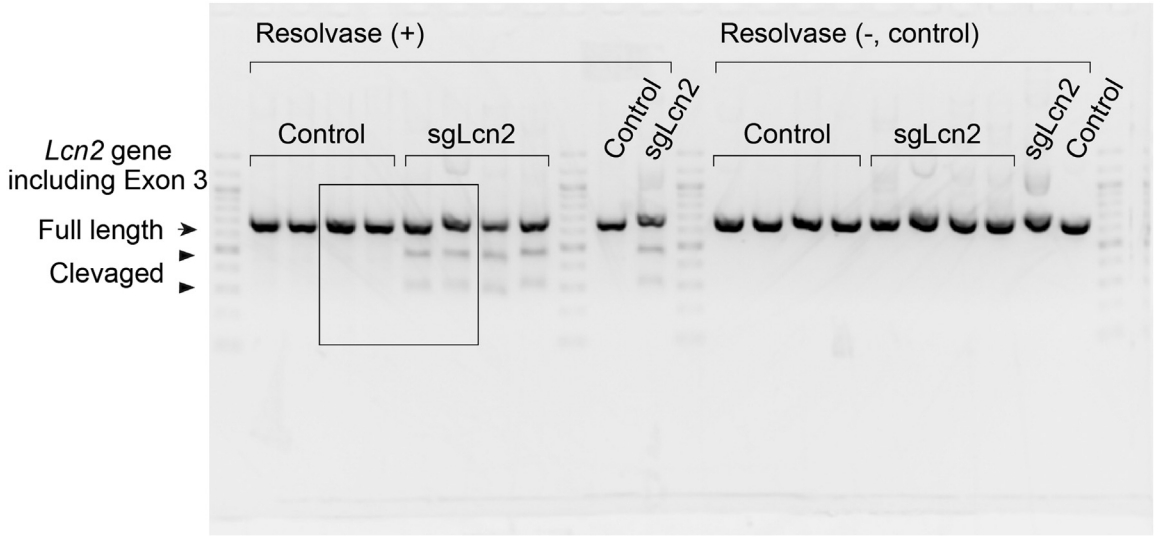

FIG E5. Full image of Fig 4, *D*. Gel image for detection of genome editing in sorted SDH astrocytes. The *square* indicates the region shown in Fig 4, *D*. The *top arrow* indicates uncleaved *Lcn2* DNA, and the 2 *arrowheads* indicate cleaved *Lcn2* DNA by using resolvase treatment. Any cleaved bands were not detected without the resolvase treatment.

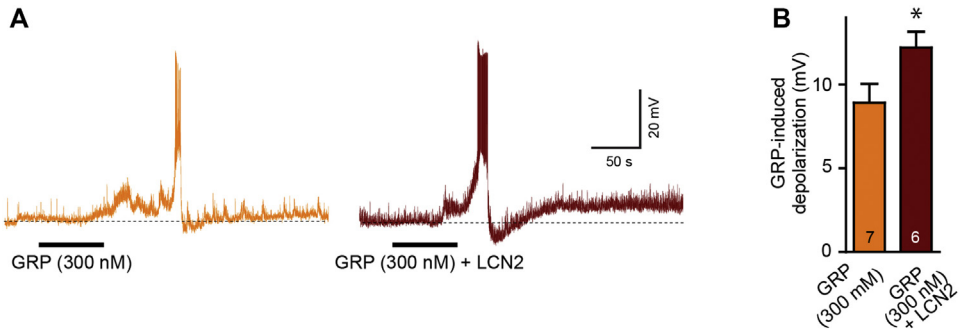

FIG E6. Effect of coapplication of LCN2 (10 nmol/L) on GRP (300 nmol/L)–induced depolarization of $GRPR^{+}$ SDH neurons in naive *Grpr-EGFP* mice. Representative traces **(A)** and averaged data **(B)** are shown (GRP, n = 7; GRP plus LCN2, n = 6). $*P < .05$.

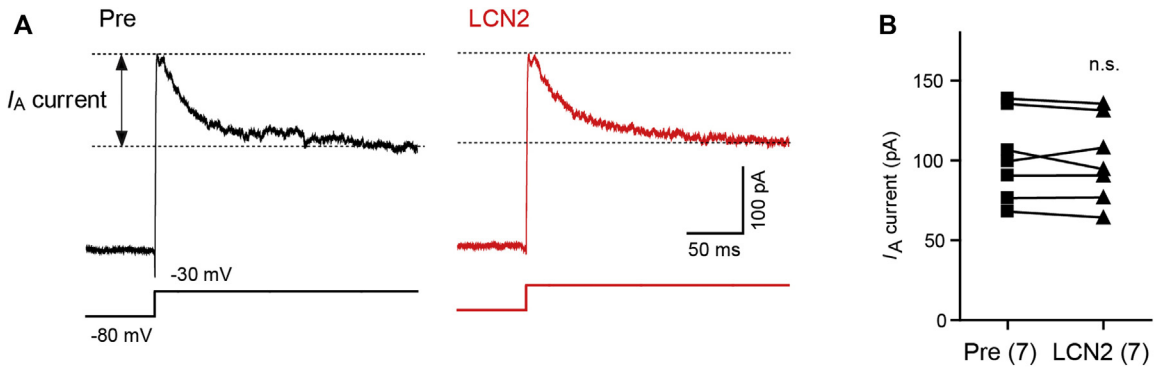

FIG E7. Effect of LCN2 (10 nmol/L) application on A-type K^+ current (I_A) current, which is mainly mediated by Kv4 channels, of $GRPR^+$ SDH neurons in naive *Grpr-EGFP* mice. Representative traces **(A)** and averaged data **(B)** are shown (n = 7).